ACS APPLIED MATERIALS & INTERFACES

Research Article

www.acsami.org

Furfural-Induced Hydrothermal Synthesis of ZnO@C Gemel Hexagonal Microrods with Enhanced Photocatalytic Activity and Stability

Peng Zhang,[†] Beibei Li,[†] Zongbin Zhao,[†] Chang Yu,[†] Chao Hu,[†] Shengji Wu,[‡] and Jieshan Qiu*[,†]

[†]Carbon Research Laboratory, Liaoning Key Lab for Energy Materials and Chemical Engineering, State Key Lab of Fine Chemicals, School of Chemical Engineering, Dalian University of Technology, Dalian 116024, China

[‡]College of Materials & Environmental Engineering, Faculty of Environmental Science and Technology, Hangzhou Dianzi University, Xiasha Higher Education Zone, Hangzhou 310018, China

Supporting Information

ABSTRACT: Here we report the synthesis of ZnO@C coaxial gemel hexagonal microrods with a thin hydrothermal carbon (HTC) layer on their surface by a facile one-step hydrothermal method with furfural as the carbon precursor. The furfural has a unique dual role, which not only induces the nucleation of ZnO in the initial stage of hydrothermal process, but also forms a thin HTC layer deposited on the ZnO surface. The thickness of the surface HTC layer increases with the hydrothermal time until 16 h under the conditions adopted in the present study. It has been found that the HTC layer has resulted in a significant improvement in the photocatalytic activities and photostabilities of the ZnO@C microrods for the UV-irradiated photodegradation of methylene blue solution. The mechanism involved in the process is proposed and discussed in terms of the photodegradation scheme and the properties of the ZnO@C microrods.

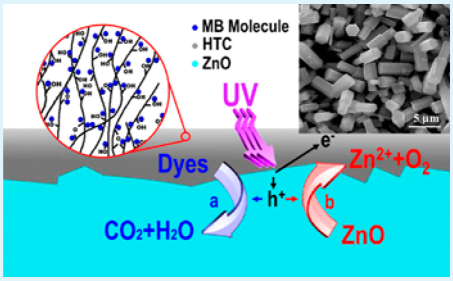

KEYWORDS: *furfural, ZnO, photocatalysis, photocorrosion, hydrothermal synthesis*

INTRODUCTION

In the past decades, the environmental problems resulting from organic pollutants discharged from textile and fine chemical industries have drawn much attention. How to effectively remove and degrade these pollutants remains a big challenge. It has been demonstrated that many metal oxide semiconductors with a large band gap are capable of catalyzing the decomposition of the organic pollutants under UV light irradiation.[1−3] Among various semiconductor photocatalysts, ZnO and TiO_2 are two ideal candidates owing to their high catalytic activity, low cost, and environmental sustainability.[4] In comparison with TiO_2, ZnO exhibits a higher efficiency for the photocatalytic degradation of some dyes in aqueous solutions.[5−9] By combining ZnO with other compounds, it is relatively easy to design and fabricate multifunctional materials.[10−12] With this driving force behind, many novel composites have been prepared by hybridizing ZnO with other materials such as Au,[13,14] Ag,[15,16] SiO_2,[17] γ-Fe_2O_3,[18] and graphene oxide.[19] Nevertheless, the photocorrosion of ZnO that used to occur in the UV-irradiation processes leads to the destructive surface structure of the photocatalysts to some degree, which consequently results in rapid decline in photocatalytic activity of ZnO catalysts. Therefore, it is important to fabricate ZnO-type photocatalysts with high photocatalytic activity and good photostability in particular in waste water treatment.

Previous studies have shown that by hybridizing ZnO with organic compounds or carbon materials, both the photocorrosion of the ZnO catalysts and the photostability of ZnO in the UV light irradiation can be improved to some degree.[20−24] Of various carbon materials, the hydrothermal carbon (HTC) made from biomass[25,26] has attracted tremendous interests because of its simple synthesis strategy, cheap and nontoxic carbon source, and more importantly, due to its excellent combinational capability with other compounds. Up to now, many HTC-based composites have been successfully prepared and used in many fields such as energy, catalysis, and environment.[27−33] Zhu et al.[34] reported the synthesis of ZnO hybridized with graphite-like carbon by coating the glucose-derived HTC on the surface of ZnO nanoparticles, and investigated its photocatalytic activity. They found that the carbon coating functioned to impede the photocorrosion of ZnO and enhance the photostability of ZnO catalysts in UV-irradiation. In their case, the surface carbon layer has two functions in the photodegradation process, that is, as a barrier that helps to prevent the structural destruction of ZnO nanoparticles, and as a capturer that helps to catch some photogenerated holes, thus inhibit the dissolution of the surface ZnO. Despite the great progress made thus far, how to fabricate

Received: March 9, 2014
Accepted: April 23, 2014
Published: April 23, 2014

   dx.doi.org/10.1021/am501423j | ACS Appl. Mater. Interfaces 2014, 6, 8560−8566

ZnO-based photocatalysts with tuned structure and super-photocatalytic activity and stability by a simple procedure remains a big challenge.

Here, we report a simple one-step hydrothermal method to synthesize ZnO-based composite photocatalysts with a thin coating layer made of HTC. The as-made ZnO@C composites have a unique morphology, which consist of two coaxial hexagonal ZnO microrods with a varying size. The mechanism involved in the formation process and the photocatalytic properties of the ZnO@C composites have been addressed in detail. It has been found that the as-made ZnO@C gemel hexagonal microrods exhibit good photocatalytic activities and photostabilities for the degradation of methylene blue (MB) solution under UV light irradiation.

EXPERIMENTAL SECTION

1. Synthesis of ZnO@C Microrods. The hydrothermal method was employed to synthesize the ZnO@C gemel hexagonal microrods. All the reagents used in the present study were of analytical grade and used without further purification. For a typical run, 0.53 g of zinc acetate, 32 mL of ethylene glycol, and 0.15 mL of furfural were added into 32 mL of deionized water under magnetic stirring at room temperature (RT), yielding a clear solution in which all gradients were completely dissolved. Then, the clear solution was transferred into a 100 mL Teflon-lined autoclave that was maintained at 180 °C for a different period of time to make ZnO@C composites that were termed as ZnO@C-*t*, where *t* refers to the reaction time. After the reaction, the autoclave was naturally cooled back to RT, and the powderlike products were collected by filtering, washed with deionized water and absolute ethanol for three times, and then dried at 80 °C under vacuum for 3 h before test and examination.

2. Characterizations of ZnO@C Microrods. The morphology and structure of the ZnO@C gemel hexagonal microrods were characterized using scanning electron microscopy (SEM, Quanta 450), energy-dispersive X-ray spectrometry (EDX, Oxford X-Max), transmission electron microscopy (TEM, JEM-2000EX), and X-ray diffraction (XRD, Rigaku D/Max-2400X, Cu Kα irradiation, operated at 40 kV and 100 mA). Thermogravimatric analysis (TG) of the samples was performed on a Mettler Toledo DSC 822 in air, in which the samples were heated from RT to 700 °C at a heating rate of 10 °C/min. Fourier transform infrared (FTIR) spectra were measured by using a Thermo Nicolet 6700 Flex apparatus with KBr as the reference. UV−vis diffuse reflectance spectra (DRS) were recorded in a range of 200−800 nm on a Thermo Evolution 220 instrument with an integrating sphere attachment. The photoluminescence (PL) spectra were recorded at RT on a Hitachi F-7000 instrument with an excitation light of 320 nm. The Brunauer−Emmett−Teller (BET) surface area of ZnO@C microrods was measured by N_2 adsorption at 77 K (Micromeritics ASAP 2020), and the samples were degassed under vacuum at 250 °C for 5 h before the measurement.

3. Photocatalytic Experiments. The photocatalytic activities of the as-made ZnO@C composites were evaluated with the UV-irradiated degradation of MB solution at RT as the probe reaction. The UV light source was a 100 W high-pressure Hg lamp with an average light intensity of 350 mW/cm^2. For a typical run, 20 mg of the ZnO@C composite sample was put into a 50 mL quartz reactor containing 40 mL of MB aqueous solution (10 mg/L). Prior to the UV light irradiation, the mixture was magnetically stirred in dark for 30 min to let the adsorption/desorption equilibrium to be established. During the irradiation, about 2 mL of suspension was sampled from the reactor at an interval of 10 min, and centrifuged to remove the solid particles before being analyzed via a UV−vis spectrophotometer (Persee TU-1810) at 664 nm that is the maximum absorption of MB. The degradation of MB was monitored by measuring the variation of the C/C_0 ratio, where C is the absorbance of filtrates at different reaction time and C_0 is the absorbance of the initial MB solution before the reaction.

The photocatalytic stability and repeatability of the ZnO@C composites were evaluated under identical conditions as described below. For a catalyst-recycle run, the only difference in the experiment procedure was to measure the absorbance of the reaction solution only at 60 min. After the reaction was finished, the concerned catalysts were collected by centrifugation, washed for three times with absolute ethanol, and dried at 80 °C under vacuum for examination and reuse.

RESULTS AND DISCUSSION

Figure 1 is the XRD patterns of the as-made ZnO@C composites, showing the featured peaks corresponding to the

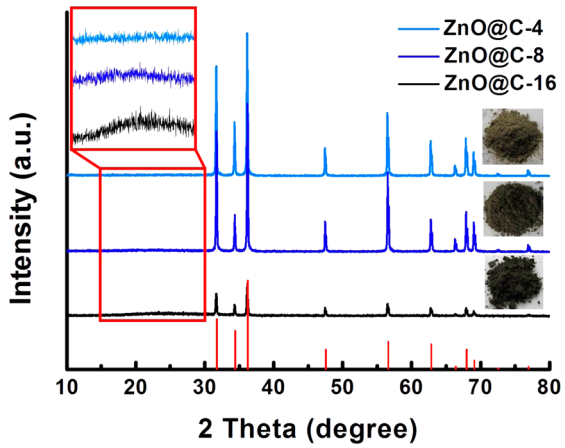

Figure 1. XRD patterns of ZnO@C composites. The inset on the left is the magnified XRD patterns from 15° to 30°, and the right inset is the digital images of the ZnO@C samples.

wurtzite structure of ZnO (*P*63*mc*, a = 3.2495, c = 5.2069, JCPDS no. 36-1451) and a broad peak in a range of 15°−30° (left inset in Figure 1). It is interesting to note that the intensity of the broad peak increases with the time of the hydrothermal reaction, suggesting that the HTC content in the ZnO@C composites increases with the reaction time, and the difference in HTC content results in a change in color of the ZnO@C composites, as shown in right inset of Figure 1.

Figure 2a is the typical SEM image of ZnO@C-16 that is made of two coaxial hexagonal rods with a different size, of which the magnified SEM image is shown in Figure 2b, revealing that the diameter of the ZnO rods is similar, but the length varies to a great degree. This is interesting, and implies that the ZnO@C microrods grow along the vertical axis in the hydrothermal process. The typical TEM image of the ZnO@C-16 (Figure 2c) shows clearly that the ZnO@C composites have a core/shell structure with the surface being coated by a HTC layer, and for the ZnO@C-16 the HTC coating layer has a thickness of ca. 5−10 nm. Figure 2d is the EDX spectrum of ZnO@C-16 with a BET surface area of 6.6 m^2/g, in which three strong peaks corresponding to C, O, and Zn species can be seen clearly, evidenced the formation and presence of HTC layers on the ZnO surface. This is in good agreement with XRD results of the ZnO@C-16 discussed above.

In the present work, furfural was used as the carbon source, which is the precursor of the thin HTC layer on the surface of ZnO rods, as reported in other hydrothermal processes with furfural as the carbon source.[35,36] We have made efforts to figure out the role played by furfural on the formation of the ZnO@C microrods. The results showed that when furfural was absent, only light yellow liquid was obtained. All of the information available now suggests that the furfural plays an

dx.doi.org/10.1021/am501423j | ACS Appl. Mater. Interfaces 2014, 6, 8560−8566

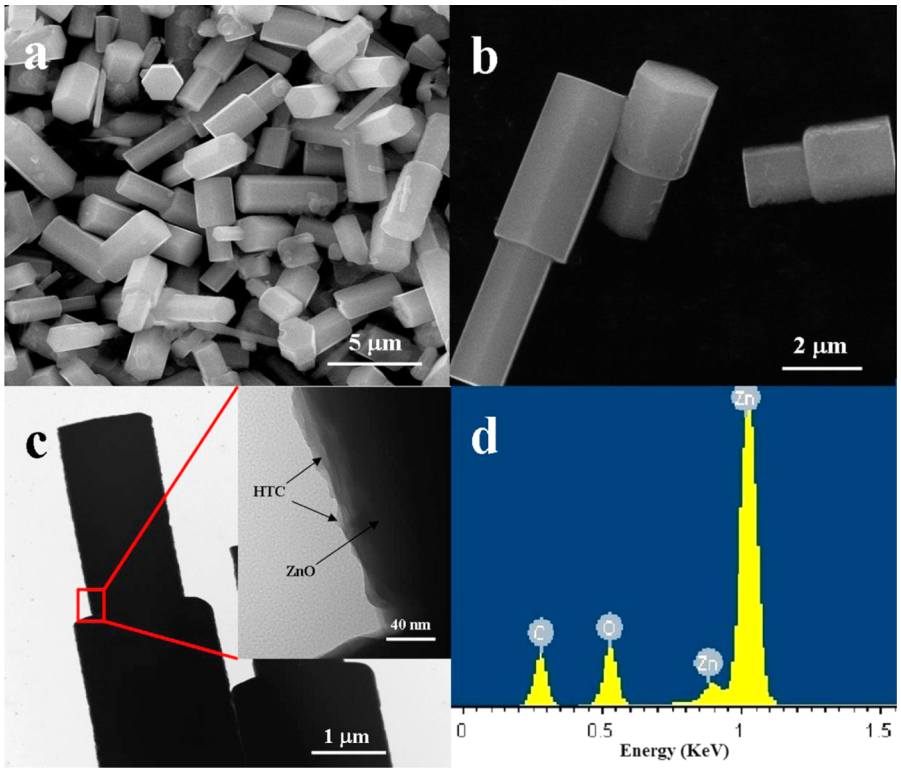

Figure 2. (a) Typical SEM image; (b) magnified SEM image; (c) TEM images; and (d) EDX analysis of ZnO@C-16.

important role in the formation of the ZnO@C composites; that is, at the initial stage of the hydrothermal process, HTC oligomers are firstly formed due to the polymerization of furfural molecules, which subsequently induce the hydrolysis of zinc acetate and the nucleation of ZnO.

In order to figure out how the ZnO@C microrods were formed, a series of experiments were performed by varying the hydrothermal reaction time. In the early reaction stage with a time of 0.25 h, only a little amount of irregular blocks were obtained, as shown in Figure S1 (Supporting Information). When the reaction time increased to 0.5 h, the products with rudimental gemel coaxial hexagonal microrods structure were obtained (Figure S2), also with a plenty of irregular blocks. As the reaction time further increased to 4 h, uniform gemel coaxial hexagonal microrods (termed as ZnO@C-4) can be observed (Figure S3a), which are not perfect, and have some defects on the surface. The TEM examination of ZnO@C-4 (Figure S3b) reveals that little HTC is coated on the ZnO surface. When the hydrothermal reaction time increased to 8 h, the morphology of the products (termed as ZnO@C-8) is very similar to the ZnO@C-16, as can be seen in Figure S4a. Figure S4b shows that the surface of ZnO@C-8 is coated with some HTC. All of the experimental results suggest that in the hydrothermal process adopted in the present study, the deposition or coating of the thin HTC layer takes place after the formation of ZnO microrods. However, when the reaction time was over 16 h, some unwanted byproducts such as colloidal carbon spheres[25,26] were formed, leading to a mixture of the ZnO@C microrods (termed as ZnO@C-24) and colloidal carbon spheres, and the ZnO@C-24 has more defects on the surface than other ZnO@C microrods obtained in less than 24 h, as shown in Figure S5.

All of the available information leads one to propose a possible formation scheme of the ZnO@C gemel hexagonal microrods, in which four steps are involved, as shown in Scheme 1: (a) In step one, at the beginning of the hydrothermal process, furfural molecules are firstly dehydrated and polymerized, resulting in HTC oligomers. (b) In step two, the HTC oligomers induce the hydrolysis of zinc acetate and the nucleation of amorphous ZnO. (c) In step three, as the reaction time increases further, the amorphous ZnO formed in the second step will grow quickly, resulting in the gemel coaxial hexagonal ZnO microrods with a different size. In this process, a small amount of HTC is also formed and hybridized into ZnO, resulting in many surface defects on the ZnO microrods. (d) In step four, in the final synthesis stage of gemel coaxial hexagonal ZnO@C microrods, a thin HTC layer is formed and deposited onto the surface of ZnO microrods. Due to the coating of thin HTC layer and the Ostwald ripening of ZnO, the surface defects of ZnO decrease gradually, evidenced by the PL results discussed below.

Scheme 1. Illustration of the Formation Process of the ZnO@C Gemel Hexagonal Microrods

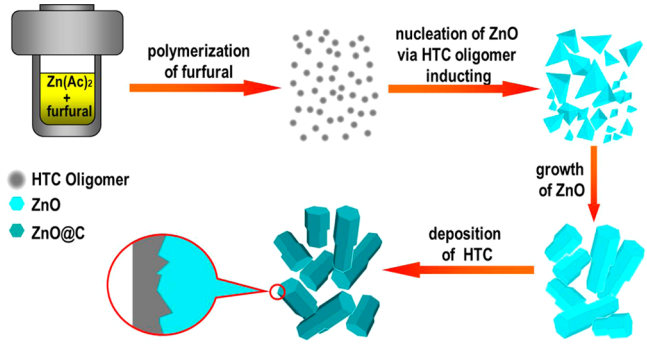

dx.doi.org/10.1021/am501423j | ACS Appl. Mater. Interfaces 2014, 6, 8560−8566

The content of HTC in the as-made ZnO@C composites was analyzed by TG analysis, of which the results are shown in Figure 3. It is believed that the slight mass losses below 220 °C

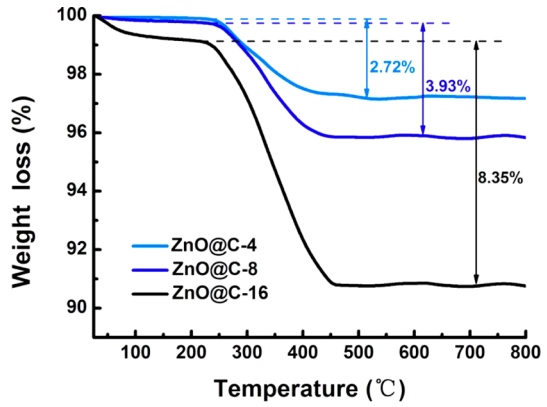

Figure 3. TG analysis of ZnO@C composites.

are due to the removal of water and gas in the samples, while the fast drop in mass loss from 220 to 450 °C is due to the combustion of the HTC on the surface. The TG analysis shows that the weight percentage of the HTC content in ZnO@C-4, ZnO@C-8, and ZnO@C-16 is 2.72, 3.93, and 8.35%, respectively.

The as-made ZnO@C composites was also analyzed by FTIR, of which the FTIR spectra are shown in Figure S6, showing characteristic peaks at ca. 500, 3500, 1700, and 1600 cm^{-1} which are assigned to the stretching vibration of Zn−O,[10] the stretching vibration of O−H, and the stretching vibrations of C−O and C═O of COO^- group, respectively.[26] This suggests that both ZnO and HTC are present in all ZnO@C composites. In comparison with ZnO@C-4 and ZnO@C-8, the FTIR peaks of ZnO@C-16 decrease dramatically in intensity, and shift in the absorption wavelength, which are probably due to the strong interaction between ZnO and HTC in the ZnO@C-16.

UV−vis diffuse reflectance spectroscopy (DRS) was employed to probe the optical properties of the ZnO@C gemel hexagonal microrods, of which the results are shown in Figure 4. Obviously, besides the strong absorption at 390 nm from the fundamental absorption edge of ZnO, a full visible absorption is observed in the UV−vis DRS of the ZnO@C composites.[19,34] In good agreement with digital photographs,

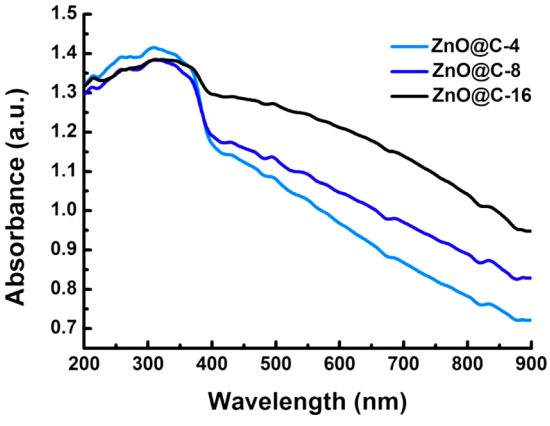

Figure 4. UV−vis DRS of ZnO@C composites.

the intensity of the visible absorbance of the ZnO@C composites increases with the increasing HTC content. However, the absorption edge and intensity do not significantly change, indicating a neglected effect of the coating HTC layer on the band gap energy and UV absorption of the ZnO@C microrods.

Figure 5 is the room temperature PL spectra of ZnO@C composites at an excitation wavelength of 320 nm. For all of

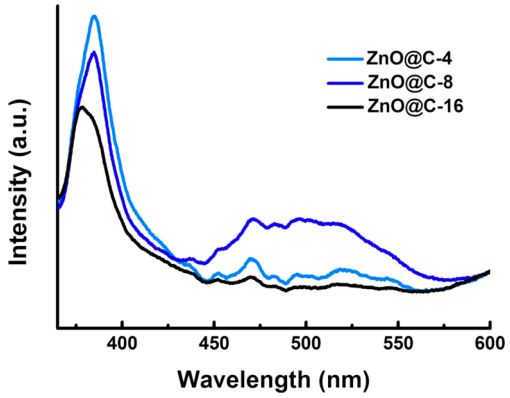

Figure 5. Room temperature PL spectra of ZnO@C composites (excited at 320 nm).

the ZnO@C composites, both a strong UV emission at 390 nm and a weak visible emission in the range of 450-550 nm can be observed. It is well known that the UV emission is due to the near band edge transition, while the visible emission is due to the transition in defect states.[4,17] Therefore, the decreasing UV emission from ZnO@C-4 to ZnO@C-16 suggests that the recombined rate of photogenerated electrons and holes becomes slower as the HTC content increases in the ZnO@C composites, implying that the photogenerated electrons on the surface of ZnO are successfully transferred to the HTC layer and the lifetime of the photogenerated holes is prolonged. Meanwhile, the ZnO@C-16 has the weakest visible emission, indicating the least defects on the ZnO surface. With all of the information mentioned above in mind, one can envision that the thin HTC layer would enhance the photocatalytic activities of the ZnO@C microrods to some degree.

The photocatalytic performance of the ZnO@C composites was evaluated by photodegrading MB solution that is a typical organic pollutant from the textile industry. Figure 6 shows the C/C_0 variation of MB in the solution under the UV light irradiation during the degradation process. Obviously, all of the ZnO@C composites exhibit good photocatalytic activities. The blank experiment in the absence of ZnO@C composites shows that there is self-photodegradation of MB, but not much. The photocatalytic activities of the ZnO@C composites increase with the increasing HTC content, and the ZnO@C-16 composite shows the best photocatalytic performance, evidenced by the fact that nearly 100% of the MB has been degraded in 40 min. The absorbance variation of MB solution in different time is shown in Figure S7. These results are in perfect agreement with the photoluminescence results discussed above, evidenced the significant improvement to the photocatalytic activity of ZnO@C composites due to the coated thin HTC layer.

The photostability of ZnO is one of the main concerns for their practical use. We have studied the photostability of ZnO@C microrods by recovering and reusing three ZnO@C

dx.doi.org/10.1021/am501423j | ACS Appl. Mater. Interfaces 2014, 6, 8560−8566

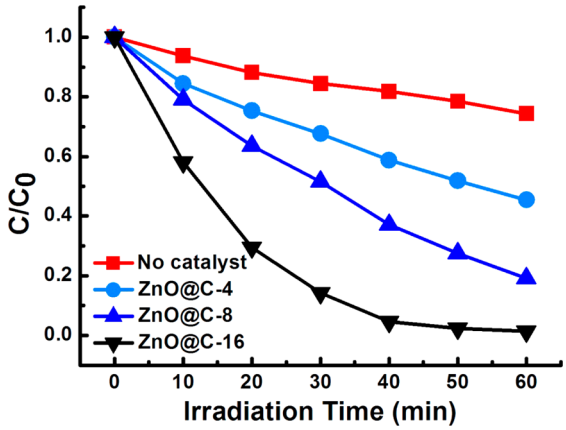

Figure 6. UV-irradiated photocatalytic degradation of MB without and with ZnO@C composites.

composite catalysts. Figure 7 shows the photodegradation performance of the ZnO@C composites that were used

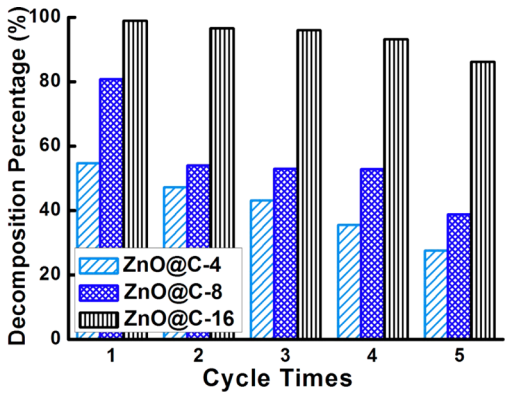

Figure 7. Photodegradation performance of ZnO@C composites in five cycles under UV light irradiation.

repeatedly five times under UV light irradiation for 60 min. Compared with ZnO@C-4 and ZnO@C-8, ZnO@C-16 exhibits a better photostability with a decomposition ratio remaining at over 90% even after five cycles. This also suggests that the photostability of ZnO@C composites has been greatly improved due to the hybridized HTC coating layer on the ZnO surface.

It is well known that in the photocatalytic process, ZnO is excited to produce electrons (e^-) and holes (h^+) under the irradiation of UV light.[4,17] The photogenerated holes will rapidly react with dye molecules absorbed on the surface of ZnO (Scheme 2, reaction a) and make them decompose quickly.[34] At the same time, the photogenerated holes are trapped by ZnO (Scheme 2, reaction b) in aqueous phase,[34] which results in the fast expulsion of Zn^{2+} from the catalyst surface into the solution. This kind of ZnO photocorrosion would destroy its surface structure to some extent, and results in the decline of photocatalytic activity of ZnO. To avoid this, reaction (a) in Scheme 2 needs to speed up, while reaction (b) must be restrained. And by this balanced strategy, one can expect the improvement both in the photocatalytic activity and in the photostability of ZnO photocatalysts.

The UV−vis DRS and PL results discussed above have shown that the surface HTC layer on the ZnO@C composites does not affect the UV light absorption but, instead, successfully prolongs the lifetime of photogenerated holes, all of which contribute to enhance the photocatalytic activity of the ZnO@C composites. On the other hand, it has been found that the HTC materials with oxygen-containing groups on their surface have great absorption capacity for organic molecules.[27,37] Because of this, in comparison to uncoated ZnO, the ZnO@C microrods will attract more dye molecules onto their surface, as shown in inset of Scheme 2. In the reaction process, more photogenerated holes will be consumed by the dye molecules under the UV light, which will speed up the reaction (a), thus enhancing the photocatalytic activities of the ZnO@C microrods. Meanwhile, the accelerated reaction (a) will consequentially decrease the rate of reaction (b), and this will impede the photocorrosion of ZnO catalysts, thus improving the photostability of the ZnO@C microrods. In a word, the coated thin HTC layer on the ZnO surface has greatly contributed to improve both photocatalytic activity and photostability of the ZnO@C gemel hexagonal microrods.

CONCLUSIONS

In summary, ZnO@C gemel coaxial hexagonal microrods with a thin HTC layer coated on the surface have been synthesized

Scheme 2. Possible Scheme of Photocatalytic Degradation of MB Molecules and Photocorrosion of the ZnO@C Gemel Hexagonal Microrods

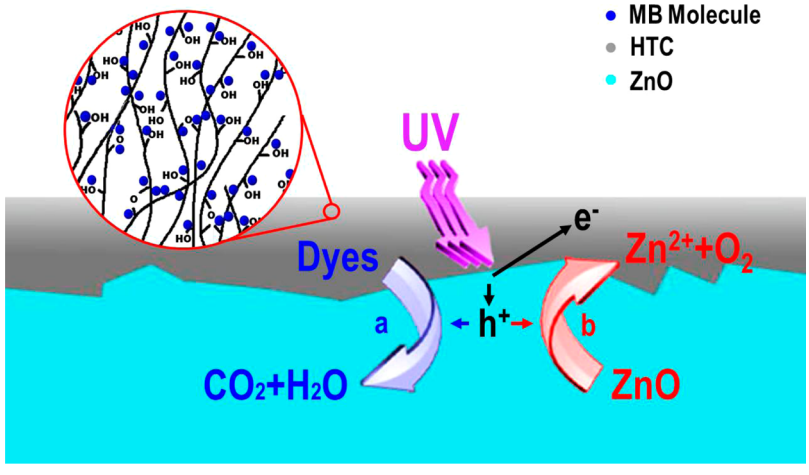

dx.doi.org/10.1021/am501423j | ACS Appl. Mater. Interfaces 2014, 6, 8560−8566

by a hydrothermal method with furfural as the carbon source. The results have shown that the coated HTC layer helps to greatly enhance the photocatalytic activity and photostability of the ZnO@C microrods for the UV-irradiated photodegradation of MB solution, and the photocatalytic properties vary with the thickness of the HTC layers to some degree. For three ZnO@C microrods (ZnO@C-4, ZnO@C-8, and ZnO@C-16) made at different times, the ZnO@C-16 has exhibited the best photocatalytic activity, evidenced by the highest photocatalytic activity for the fresh catalyst and the high efficiency of photodegradation for reused ones. The superb photocatalytic performance of the ZnO@C gemel hexagonal microrods makes them hold promise as candidates for efficient photocatalytic degradation of organic pollutants.

■ ASSOCIATED CONTENT

Supporting Information

SEM images of ZnO@C-0.25, ZnO@C-0.5, ZnO@C-4, ZnO@C-8, and ZnO@C-24. TEM images of ZnO@C-4 and ZnO@C-8. FTIR spectra of ZnO@-4, ZnO@C-8, and ZnO@C-16. UV−vis absorbance of the MB solution at different photocatalytic reaction time over ZnO@C-16 under UV irradiation. This material is available free of charge via the Internet at http://pubs.acs.org.

■ AUTHOR INFORMATION

Corresponding Author

*Mailing address: Carbon Research Laboratory, Liaoning Key Lab for Energy Materials and Chemical Engineering, State Key Lab of Fine Chemicals, School of Chemical Engineering, Dalian University of Technology, No. 2 Linggong Road, High Tech-Zone, Dalian 116024, Liaoning, China. E-mail: jqiu@dlut.edu.cn. Tel: +86-411-84986024.

Notes

The authors declare no competing financial interest.

■ ACKNOWLEDGMENTS

This work was partly supported by NSFC (No. 21361162004, 21336001), the Doctoral Program of Higher Education of China (No. 20120041110020), Zhejiang Provincial Natural Science Foundation of China (No. LY12E06001), and Science and Technology Planning Project of Zhejiang Province of China (No. 2013C31016).

■ REFERENCES

(1) Chen, X.; Shen, S.; Guo, L.; Mao, S. S. Semiconductor-Based Photocatalytic Hydrogen Generation. *Chem. Rev.* **2010**, *110*, 6503−6570.

(2) Fox, M. A.; Dulay, M. T. Heterogeneous Photocatalysis. *Chem. Rev.* **1993**, *93*, 341−357.

(3) Hoffmann, M. R.; Martin, S. T.; Choi, W. Y.; Bahnemann, D. W. Environmental Applications of Semiconductor Photocatalysis. *Chem. Rev.* **1995**, *95*, 69−96.

(4) Li, Y.; Xie, W.; Hu, X.; Shen, G.; Zhou, X.; Xiang, Y.; Zhao, X.; Fang, P. Comparison of Dye Photodegradation and Its Coupling with Light-to-Electricity Conversion over TiO_2 and ZnO. *Langmuir* **2010**, *26*, 591−597.

(5) Ye, C.; Bando, Y.; Shen, G.; Golberg, D. Thickness-Dependent Photocatalytic Performance of ZnO Nanoplatelets. *J. Phys. Chem. B* **2006**, *110*, 15146−15151.

(6) Wang, H. Q.; Li, G. H.; Jia, L. C.; Wang, G. Z.; Tang, C. J. Controllable Preferential-Etching Synthesis and Photocatalytic Activity of Porous ZnO Nanotubes. *J. Phys. Chem. C* **2008**, *112*, 11738−11743.

(7) Sun, T. J.; Qiu, J. S.; Liang, C. H. Controllable Fabrication and Photocatalytic Activity of ZnO Nanobelt Arrays. *J. Phys. Chem. C* **2008**, *112*, 715−721.

(8) Liu, Y.; Shi, J.; Peng, Q.; Li, Y. Self-Assembly of ZnO Nanocrystals into Nanoporous Pyramids: High Selective Adsorption and Photocatalytic Activity. *J. Mater. Chem.* **2012**, *22*, 6539−6541.

(9) Guo, M. Y.; Ng, A. M. C.; Liu, F.; Djurišić, A. B.; Chan, W. K.; Su, H.; Wong, K. S. Effect of Native Defects on Photocatalytic Properties of ZnO. *J. Phys. Chem. C* **2011**, *115*, 11095−11101.

(10) Xiao, F.; Wang, F.; Fu, X.; Zheng, Y. A Green and Facile Self-Assembly Preparation of Gold Nanoparticles/ZnO Nanocomposite for Photocatalytic and Photoelectrochemical Applications. *J. Mater. Chem.* **2012**, *22*, 2868−2877.

(11) Ahmad, M.; Pan, C. F.; Gan, L.; Nawaz, Z.; Zhu, J. Highly Sensitive Amperometric Cholesterol Biosensor Based on Pt-Incorporated Fullerene-Like ZnO Nanospheres. *J. Phys. Chem. C* **2010**, *114*, 243−250.

(12) Aguirre, M. E.; Rodríguez, H. B.; San Román, E.; Feldhoff, A.; Grela, M. A. Ag@ZnO Core−Shell Nanoparticles Formed by the Timely Reduction of Ag^+ Ions and Zinc Acetate Hydrolysis In *N,N*-Dimethylformamide: Mechanism of Growth and Photocatalytic Properties. *J. Phys. Chem. C* **2011**, *115*, 24967−24974.

(13) Li, P.; Wei, Z.; Wu, T.; Peng, Q.; Li, Y. Au-ZnO Hybrid Nanopyramids and Their Photocatalytic Properties. *J. Am. Chem. Soc.* **2011**, *133*, 5660−5663.

(14) Ahmad, M.; Shi, Y.; Nisar, A.; Sun, H.; Shen, W.; Wei, M.; Zhu, J. Synthesis of Hierarchical Flower-Like ZnO Nanostructures and Their Functionalization by Au Nanoparticles for Improved Photocatalytic and High Performance Li-Ion Battery Anodes. *J. Mater. Chem.* **2011**, *21*, 7723−7729.

(15) Zheng, Y.; Zheng, L.; Zhan, Y.; Lin, X.; Zheng, Q.; Wei, K. Ag/ZnO Heterostructure Nanocrystals: Synthesis, Characterization, and Photocatalysis. *Inorg. Chem.* **2007**, *46*, 6980−6986.

(16) Gu, C.; Cheng, C.; Huang, H.; Wong, T.; Wang, N.; Zhang, T. Growth and Photocatalytic Activity of Dendrite-Like ZnO@Ag Heterostructure Nanocrystals. *Cryst. Growth Des.* **2009**, *9*, 3278−3285.

(17) Wang, R.; Guo, J.; Chen, D.; Miao, Y.-E.; Pan, J.; Tjiu, W. W.; Liu, T. Tube Brush" Like ZnO/SiO_2 Hybrid to Construct a Flexible Membrane with Enhanced Photocatalytic Properties and Recycling Ability. *J. Mater. Chem.* **2011**, *21*, 19375−19380.

(18) Liu, Y.; Yu, L.; Hu, Y.; Guo, C.; Zhang, F.; Lou, X. W. A Magnetically Separable Photocatalyst Based on Nest-Like Gamma-Fe_2O_3/ZnO Double-Shelled Hollow Structures with Enhanced Photocatalytic Activity. *Nanoscale* **2012**, *4*, 183−187.

(19) Luo, Q. P.; Yu, X. Y.; Lei, B. X.; Chen, H. Y.; Kuang, D. B.; Su, C. Y. Reduced Graphene Oxide-Hierarchical ZnO Hollow Sphere Composites with Enhanced Photocurrent and Photocatalytic Activity. *J. Phys. Chem. C* **2012**, *116*, 8111−8117.

(20) Xu, T.; Zhang, L.; Cheng, H.; Zhu, Y. Significantly Enhanced Photocatalytic Performance of ZnO via Graphene Hybridization and the Mechanism Study. *Appl. Catal. B* **2011**, *101*, 382−387.

(21) Wang, Y.; Shi, R.; Lin, J.; Zhu, Y. Enhancement of Photocurrent and Photocatalytic Activity of ZnO Hybridized with Graphite-Like C_3N_4. *Energy Environ. Sci.* **2011**, *4*, 2922−2929.

(22) Li, Y. Z.; Zhou, X.; Hu, X. L.; Zhao, X. J.; Fang, P. F. Formation of Surface Complex Leading to Efficient Visible Photocatalytic Activity and Improvement of Photostabilty of ZnO. *J. Phys. Chem. C* **2009**, *113*, 16188−16192.

(23) Fu, H.; Xu, T.; Zhu, S.; Zhu, Y. Photocorrosion Inhibition and Enhancement of Photocatalytic Activity for ZnO via Hybridization with C_{60}. *Environ. Sci. Technol.* **2008**, *42*, 8064−8069.

(24) Comparelli, R.; Fanizza, E.; Curri, M. L.; Cozzoli, P. D.; Mascolo, G.; Agostiano, A. UV-Induced Photocatalytic Degradation of Azo Dyes by Organic-Capped ZnO Nanocrystals Immobilized onto Substrates. *Appl. Catal. B* **2005**, *60*, 1−11.

(25) Titirici, M. M.; Antonietti, M.; Baccile, N. Hydrothermal Carbon from Biomass: A Comparison of the Local Structure from Poly- to Monosaccharides and Pentoses/Hexoses. *Green Chem.* **2008**, *10*, 1204−1212.

(26) Sun, X. M.; Li, Y. D. Colloidal Carbon Spheres and Their Core/Shell Structures with Noble-Metal Nanoparticles. *Angew. Chem., Int. Ed.* **2004**, *43*, 597−601.
(27) Chen, L. F.; Lang, H. W.; Lu, Y.; Cui, C. H.; Yu, S. H. Synthesis of an Attapulgite Clay@Carbon Nanocomposite Adsorbent by a Hydrothermal Carbonization Process and Their Application in the Removal of Toxic Metal Ions from Water. *Langmuir* **2011**, *27*, 8998−9004.
(28) Lou, X. W.; Chen, J. S.; Chen, P.; Archer, L. A. One-Pot Synthesis of Carbon-Coated SnO_2 Nanocolloids with Improved Reversible Lithium Storage Properties. *Chem. Mater.* **2009**, *21*, 2868−2874.
(29) Makowski, P.; Cakan, R. D.; Antonietti, M.; Goettmann, F.; Titirici, M. M. Selective Partial Hydrogenation of Hydroxy Aromatic Derivatives with Palladium Nanoparticles Supported on Hydrophilic Carbon. *Chem. Commun.* **2008**, 999−1001.
(30) Xing, L.; Qiu, J.; Liang, C.; Wang, C.; Mao, L. A New Approach to High Performance Co/C Catalysts for Selective Hydrogenation of Chloronitrobenzenes. *J. Catal.* **2007**, *250*, 369−372.
(31) Zhu, T.; Chen, J. S.; Lou, X. W. Glucose-Assisted One-Pot Synthesis of FeOOH Nanorods and Their Transformation to Fe_3O_4@Carbon Nanorods for Application in Lithium Ion Batteries. *J. Phys. Chem. C* **2011**, *115*, 9814−9820.
(32) Hu, Y.; Gao, X.; Yu, L.; Wang, Y.; Ning, J.; Xu, S.; Lou, X. W. Carbon-Coated CdS Petalous Nanostructures with Enhanced Photostability and Photocatalytic Activity. *Angew. Chem., Int. Ed.* **2013**, *52*, 5636−5639.
(33) Liu, Y.; Zhou, L.; Hu, Y.; Guo, C.; Qian, H.; Zhang, F.; Lou, X. W. Magnetic-Field Induced Formation of 1D Fe_3O_4/C/CdS Coaxial Nanochains as Highly Efficient and Reusable Photocatalysts for Water Treatment. *J. Mater. Chem.* **2011**, *21*, 18359−18364.
(34) Zhang, L.; Cheng, H.; Zong, R.; Zhu, Y. Photocorrosion Suppression of ZnO Nanoparticles via Hybridization with Graphite-Like Carbon and Enhanced Photocatalytic Activity. *J. Phys. Chem. C* **2009**, *113*, 2368−2374.
(35) Falco, C.; Caballero, F. P.; Babonneau, F.; Gervais, C.; Laurent, G.; Titirici, M. M.; Baccile, N. Hydrothermal Carbon from Biomass: Structural Differences between Hydrothermal and Pyrolyzed Carbons via C^{13} Solid State NMR. *Langmuir* **2011**, *27*, 14460−14471.
(36) Sevilla, M.; Fuertes, A. B. Chemical and Structural Properties of Carbonaceous Products Obtained by Hydrothermal Carbonization of Saccharides. *Chem.—Eur. J.* **2009**, *15*, 4195−4203.
(37) Sun, X. M.; Li, Y. D. Ga_2O_3 and GaN Semiconductor Hollow Spheres. *Angew. Chem., Int. Ed.* **2004**, *43*, 3827−3831.